

## Chapter 7:

# HORN SYSTEMS

### *7 Introduction*

The history of the horn as an acoustic device dates to antiquity. Early man used hollowed animal horns for signaling over long distances, and in time the horn became the basis of a number of musical instruments.

Horn loudspeakers were developed fairly early in electroacoustics and were useful primarily because of their relatively high efficiencies and the ease with which their directivity patterns could be controlled. Important work was carried out by Wentz and Thuras at Bell Laboratories in the mid 1920s, soon followed by RCA, Lansing, Altec, Jensen and Stephens.

For several decades, the development of horn systems was driven by the requirements of motion picture sound and the need for filling large spaces with fairly high sound pressure levels using power amplifiers of relatively modest output. Further refinements in horn systems during the sixties and seventies were driven by the demands of recording technology and high-level music reinforcement in outdoor venues.

Modern horn systems are characterized by high power handling capability, uniform directional control and low distortion at high output levels.

### *7.1 Horn flare profiles*

In distinction to a direct radiator, whose moving system is mass controlled and looks into a radiation resistance that rises with frequency, the horn presents a load that is resistive over a large portion of its normal passband. Figure 7-1A shows the section profiles of two horns, exponential and hyperbolic, that have been widely used in electroacoustics. As shown at *B*, the hyperbolic (Hypex) horn (Salmon 1941) exhibits a slight rise in radiation resistance just above the nominal cutoff frequency,  $f_c$ , followed by a rapid drop. While it has

been used in a number of high frequency devices, the hyperbolic horn is not normally used for midrange applications. Its application at LF has been limited, but its rise in radiation impedance could offer substantial advantages in acoustical loading at LF.

The profile of the exponential horn is shown in greater detail in Figure 7-1C. The equation for the horn's cross-sectional area, as a function of  $x$ , is given by:

$$S(x) = S_T e^{mx} \quad 7.1$$

where:  $S(x)$  = area at a distance,  $x$ , from the throat  
 $S_T$  = area of the throat, meter<sup>2</sup>  
 $e = 2.718$  (base of the natural logarithm system)  
 $m$  = flare constant, meter<sup>-1</sup>  
 $x$  = distance from the throat along horn axis, meter

The flare constant is:

$$m = 4\pi f_c / c \quad 7.2$$

where:  $f_c$  = cutoff frequency  
 $c$  = velocity of sound, meter/sec

In terms of the horn's cutoff frequency, the approximate complex load at the throat of the horn is given by:

$$Z_{AT} = (\rho_0 c / S_T) \left[ \sqrt{1 - (f_c/f)^2} + j f_c/f \right] = R_{AT} + jX_{AT} \quad 7.3$$

where:  $f$  = driving frequency  
 $\rho_0 c = 406$  mechanical ohms at standard temperature and pressure

The values of  $R_{AT}$  and  $X_{AT}$  for an infinite exponential horn are shown in Figure 7-1D. At frequencies lower than  $f_c$ , the impedance of the horn will be largely (but not entirely) reactive, and relatively little power will be transmitted. At frequencies much higher than  $f_c$ , the reactive term will become very small, and the resistive term will be dominant. For reasons having to do with size, many LF horns are used down to frequencies fairly close to cutoff.

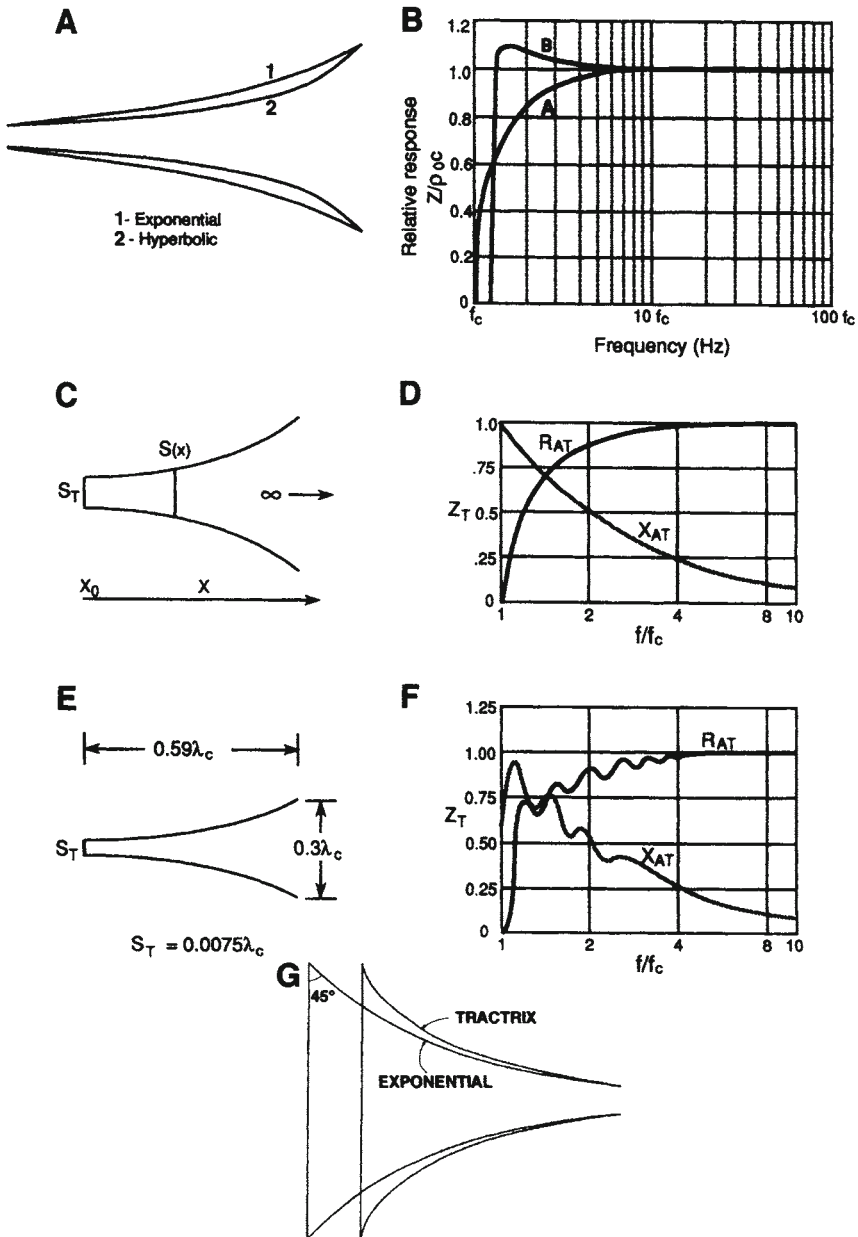


Figure 7-1. Horn profiles and impedances. Section views of exponential and hyperbolic horns (A); radiation resistance for exponential and hyperbolic horns (B); detail of an infinite exponential horn (C); approximate radiation resistance and reactance for an infinite exponential horn (D); detail of a finite exponential horn (E) radiation resistance and reactance for horn shown at E (F); tractrix and exponential profiles (G). (A through F after Beranek, 1954; G after Edgar, 1981)

HF horns, for reasons having to do with efficiency and proper driver loading, are designed to be used in the range where resistive loading is dominant.

If the circumference of the horn's mouth is greater than approximately three wavelengths of the lowest frequency to be reproduced, then the horn's impedance will behave very much like that shown in Figure 7-1D. The data shown at *E* and *F* are for a finite horn of the dimensions indicated. The ripple in the plotted curves is caused by reflections from the mouth of the horn back to the driver due to the acoustical impedance discontinuity the traveling wave sees as it passes the abrupt termination at the mouth. In these figures,  $\lambda_c$  is the wavelength of the cutoff frequency.

The normal passband of the horn is that region above which the resistive component of impedance has effectively reached its maximum value, which is equal to:

$$Z_{MT} = \rho_0 c S_T, \text{ mechanical ohms} \quad 7.4$$

where:  $S_T$  = area of the throat, square meters

HF horns are often used as high as 8 to  $10f_c$  and in the range above  $4f_c$  the radiation resistance will be that of a piston, as shown in Figure 1-6. The response will thus show the characteristic ripples in the radiation resistance above  $ka = 2$ , even in the case of the so-called infinite horn (Keele 1973).

The *tractrix* horn, developed by Voigt (1927), has earned special status among horn-enthusiasts and audiophiles. Unlike the exponential horn, whose contour is normally generated outward from the throat, the tractrix horn is fundamentally generated from the mouth back to the throat. The mouth size is scaled according to the desired LF cutoff frequency, and the throat boundary is set by the initial expansion rate that is required for the chosen cutoff frequency. As can be seen in Figure 7-1G, the initial flare rates for both exponential and tractrix horns are quite similar, and the loading characteristics of the two are similar as well.

There are two slight advantages of the tractrix horn over the exponential: the throat resistive component of impedance of the tractrix horn maintains a higher value in the neighborhood of cutoff than the exponential horn, and the bell-like flaring at the mouth contributes to maintaining broader coverage at HF.

## 7.2 The driving transducer

The transducer normally used with a horn is called a *compression driver*, and several photos and cutaway views of modern compression drivers are shown in Figure 7-2. Drivers such as these provide response from 500-800 Hz to about 20 kHz when mounted on appropriate horns. Modern drivers which are used to cover the range from about 500 Hz to 20 kHz fall generally into three size categories:

Diaphragm diameter:	Driver exit diameter:	Peak power rating:
44.5 mm (1.75")	25.4 mm (1")	40 W
76 mm (3")	38 mm (1.5")	75 W
100 mm (4")	50 mm (2")	100 W

Figure 7-3 shows a labeled section and end view of a driver of the types illustrated in Figure 7-2.

The driver design shown here was pioneered by Bell Telephone Laboratories and its associated manufacturing division, Western Electric (WE). This driver design is characterized by its unique annular slit phasing plug, which provides the necessary compression ratio between the diaphragm and the driver's outlet. Also characteristic here is the position of the diaphragm at the rear of the driver, with the signal firing through the magnetic structure to its output at the front.

### 7.2.1 Other phasing plug designs

Alternate phasing plug profiles are shown in Figure 7-4 in both end and section views. The WE design is shown at *A*. The design shown at *B* was introduced by the Lansing Manufacturing Company in the late 1930s, ostensibly as a means of working around the basic WE patent on the annular slit design. The form shown at *C* was introduced during the 1940s by the British Tannoy company in their legendary "Dual-Concentric" coaxial monitor loudspeaker, and it continues to this day.

### 7.2.2 Other driver concepts

There have been variations on the basic driver concept, as shown in Figure 7-5. The "tear-drop" design shown at *A* has only one annular path between the diaphragm, and as such it has limited high frequency capability. The multiple tear-drop design, shown at *B*, is often used in high frequency radiators. Here,

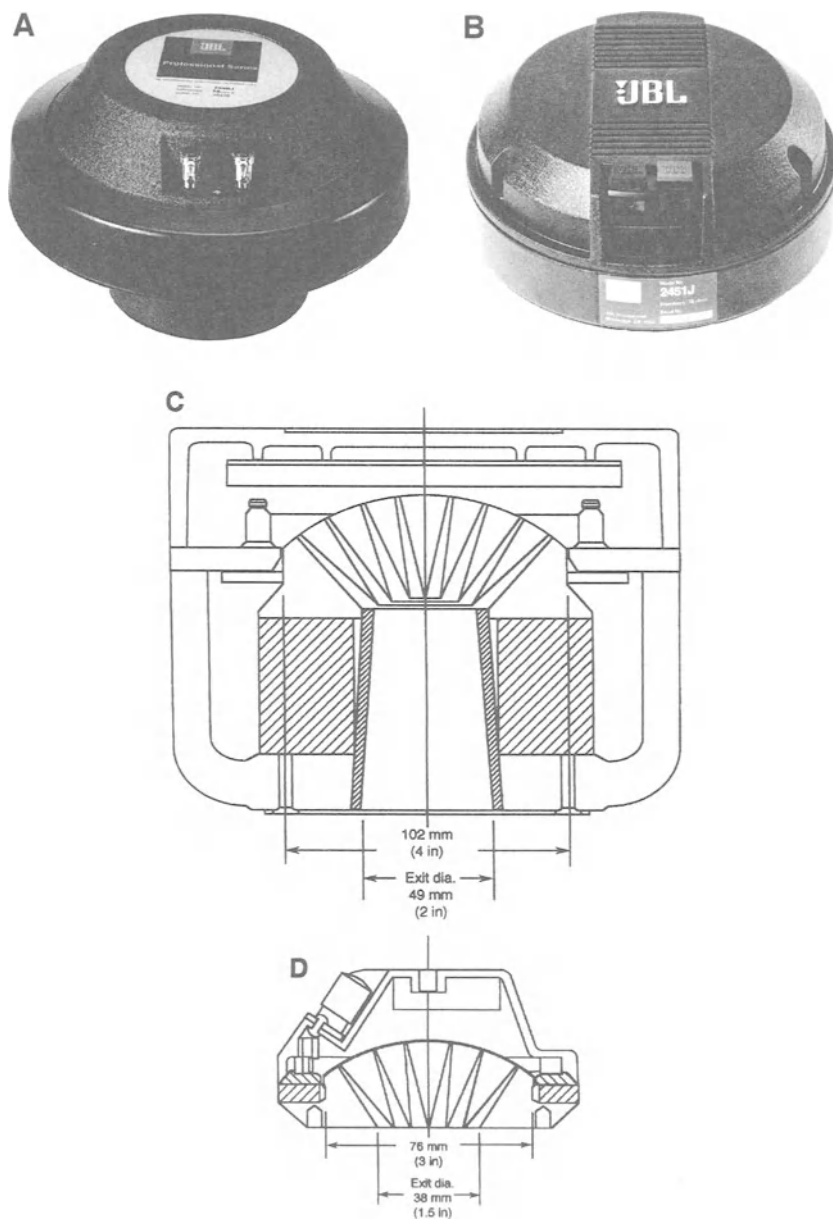


Figure 7-2. Photos and cutaway views of HF compression drivers. 100-mm diaphragm with ferrite magnet (A); 100-mm diaphragm with neodymium magnet (B); section view of 100-mm diaphragm driver with Alnico V magnet (C); section view of 76-mm diaphragm driver with neodymium magnet (D). (Data courtesy JBL)

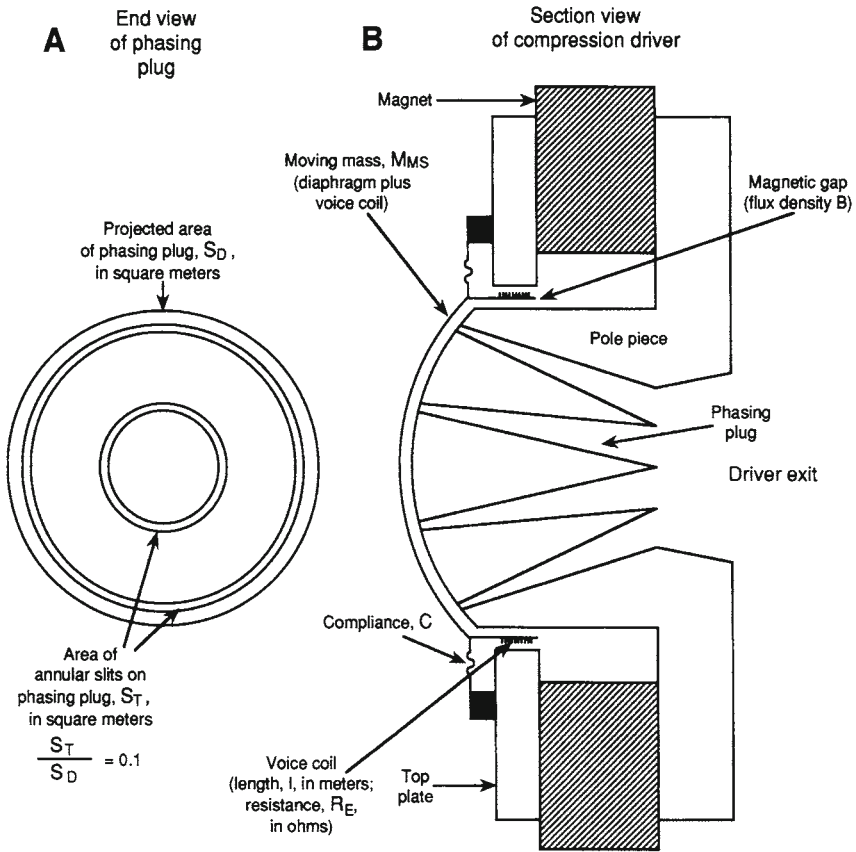


Figure 7-3. Views of a HF compression driver. Normal view of phasing plug as seen from diaphragm side (A); section view (B). (Data courtesy JBL)

the sections are circular, and the response is very much like that of the basic WE design. The design shown at *C* is basically a ring radiator in that its output originates from an annular diaphragm clamped on the inside and outside of the radiating surface. The design is normally limited to small drivers. The design shown at *D* (Voishvillo & Surupov, 1996) has a free-edged diaphragm and is clamped in the center. It is a close cousin to the Community VHF 100 design, which was introduced in the early 1990s.

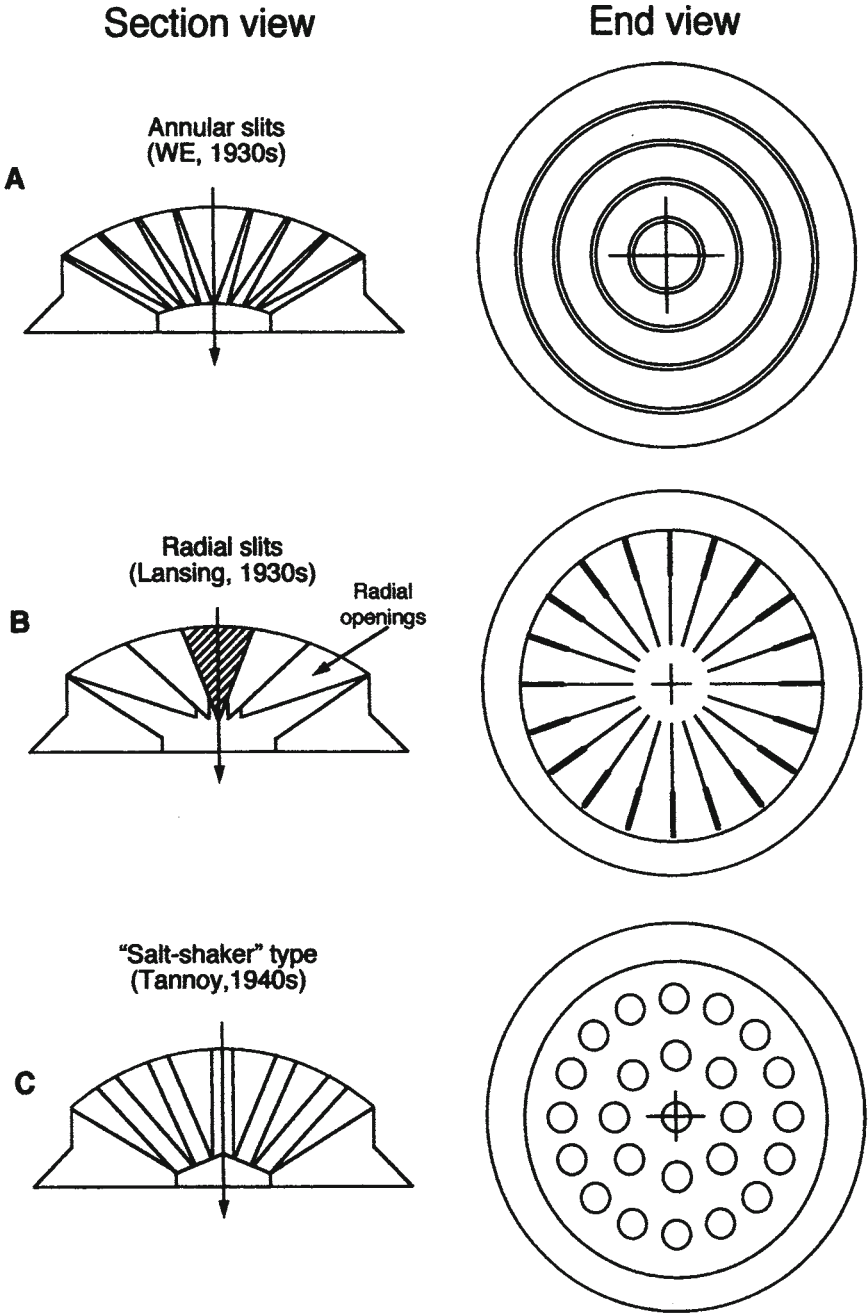


Figure 7-4. Section and end views of several types of phasing plugs.



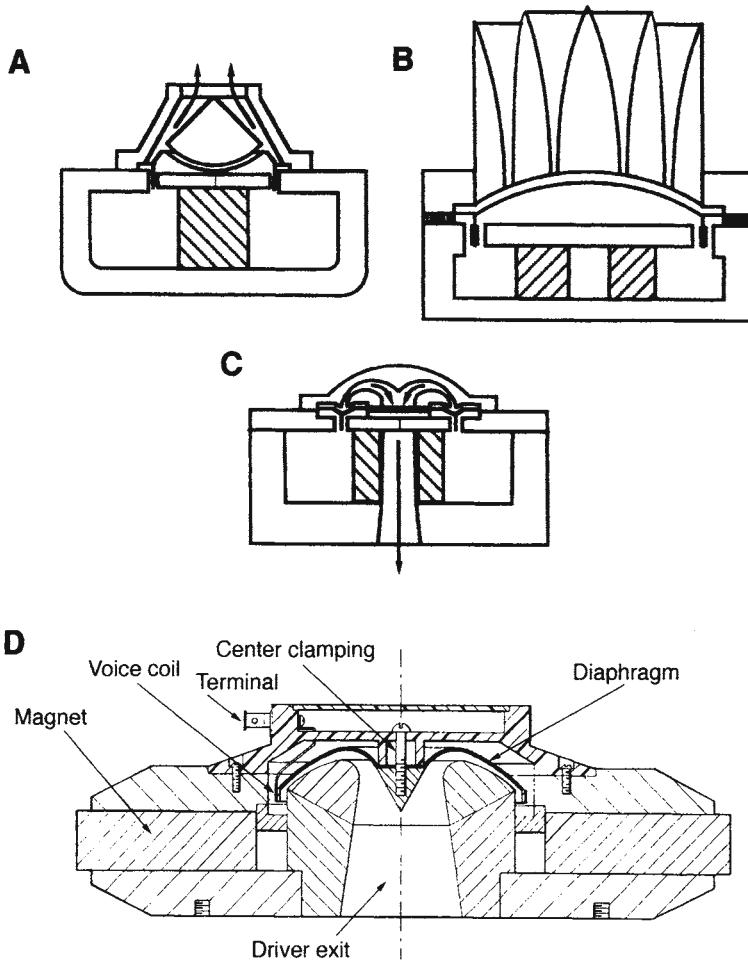


Figure 7-5. Views of other types of compression drivers. Teardrop type (A); multiple teardrop type (B); re-entrant type (C); center-clamped, free-edge type (D); two-way design (E). (Data at *D* courtesy A. Voishvillo; data at *E* courtesy BMS ElektronikGmbH)

The design shown at *E* is unique in that it contains both MF and HF sections in a two-way configuration. Both MF and HF transducers take the form of ring radiators, and an elaborate manifold (not shown in this figure) directs the two outputs to their respective channels, with no interaction between them. The frequency division between sections is at 7 kHz.

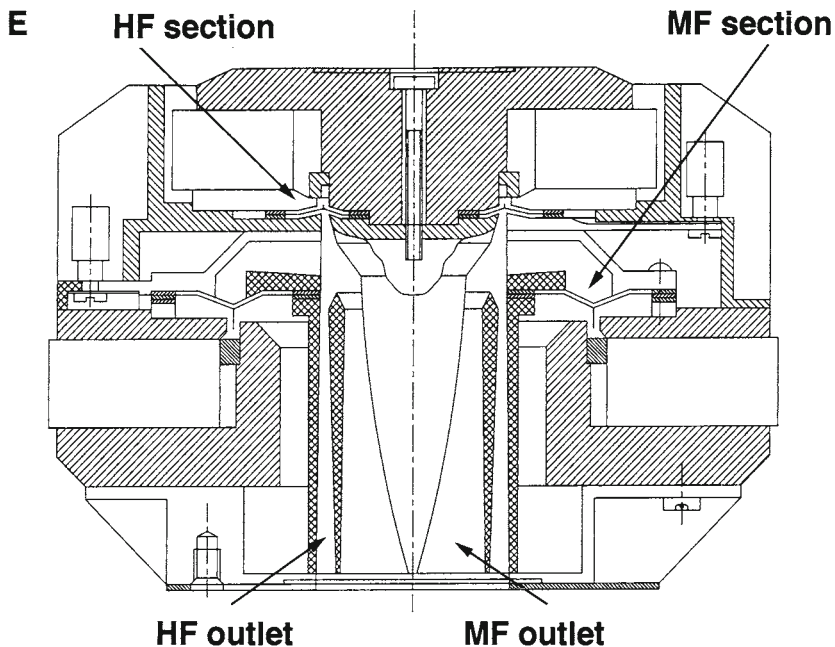


Figure 7-5. Continued.

### 7.2.3 Diaphragm compliance designs

The diaphragm designs shown in Figure 7-6A through C are normally formed from a single piece of metal by pneumatic or hydraulic drawing of the material. Aluminum, titanium, and some forms of beryllium can be shaped in this manner. In other designs, vacuum electro-deposition of beryllium is used.

The *tangential* compliance shown at A dates from the late 1920s and is still used today. Its main feature is that it provides a fairly high, well damped secondary resonance, which yields extended frequency response. The design works well with aluminum, due to the high ductility of that material.

The half-roll surround shown at B provides a rather abrupt mechanical termination at the edge of the diaphragm which results in a HF response rise followed by a sharp drop in response.

The so-called “diamond” surround shown at C consists of a number of diamond-shaped impressions pressed into the surround, resulting in a response similar to that of the tangential surround, but with less stress in the metal, and consequently greater reliability and ease of manufacture.

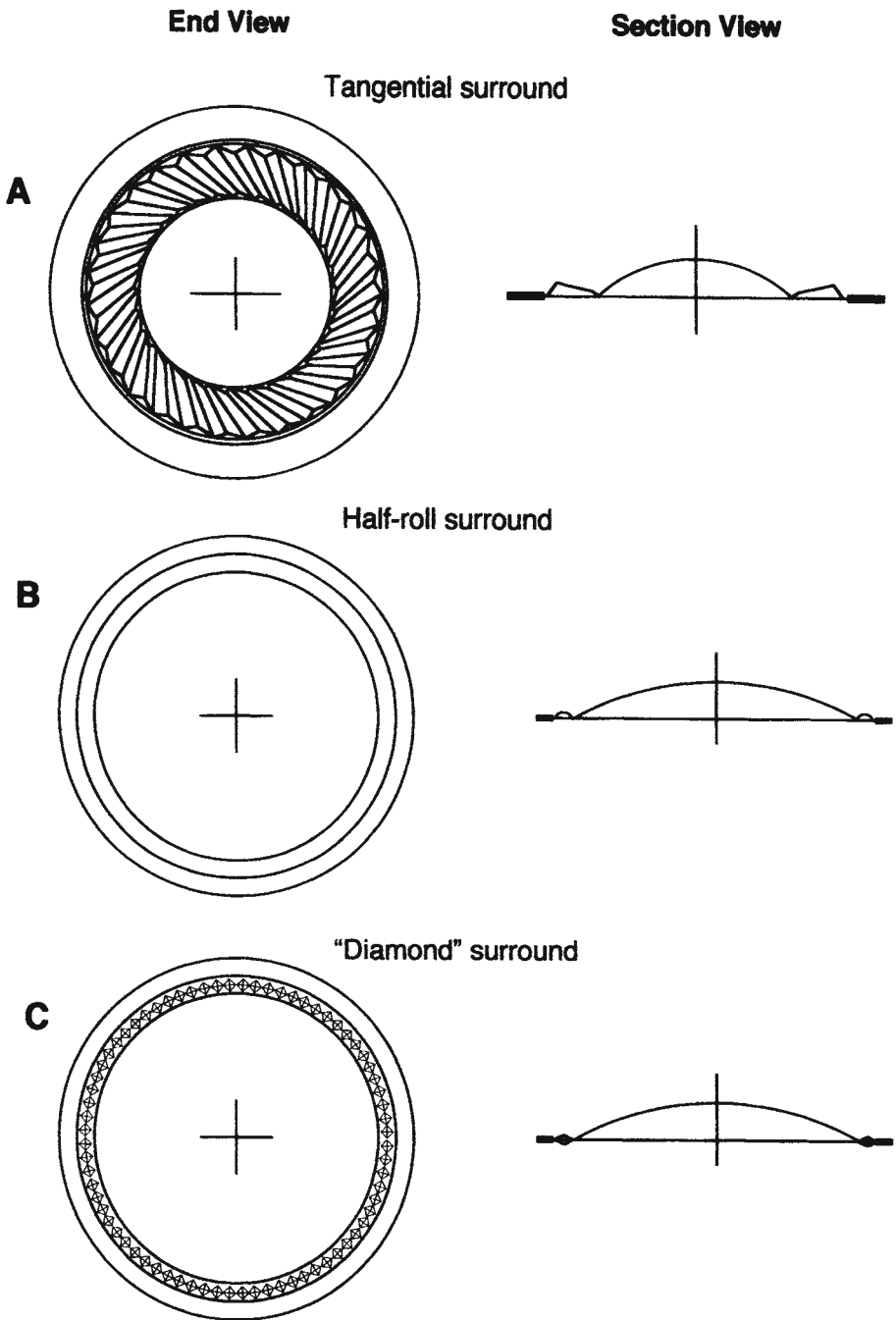


Figure 7-6. Diaphragm types. Tangential (A); half-roll (B); diamond (C); composite (D).

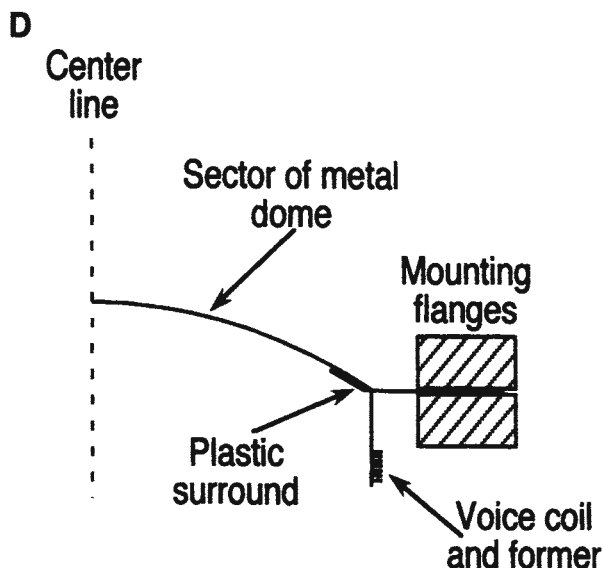


Figure 7-6. Continued.

Figure 7-6D shows a diaphragm-voice coil assembly composed of a metal diaphragm and a plastic surround structure. Designs such as these restrict the high bending motions to the plastic materials, which are far better equipped to handle them than is the metal dome itself. In construction, these designs are more difficult to make than single-piece structures, and there is likely to be more variation in unit-to-unit response. High temperature adhesives are used, along with robust plastic materials such as Kapton and various polyamids.

#### 7.2.4 Construction details

The high frequency driver is a precision device with many design tolerances in the range of  $\pm 40$  microns ( $\pm 0.001$  in). The magnetic circuit normally operates with the top plate and pole piece at or near saturation, and gap flux densities in excess of 2.0 T can be attained.

Typical HF diaphragm diameters range from about 45 to 100 millimeters. Diaphragm materials have included phenolic impregnated linen, aluminum, titanium, and beryllium. The metal diaphragms have a thickness of about 40 to 80 microns. The ideal diaphragm material for extended high frequency response is one that is rigid, of low mass, and fatigue resistant. The search for better materials continues. Diaphragm moving mass is generally quite low, and a typical value for a 100-mm diameter diaphragm/voice coil assembly is about 3.5 grams.

The diaphragm is separated from the phasing plug by a space just large enough to ensure that it will not hit the phasing plug on large excursions at lower frequencies. The annular slits in the phasing plug have a collective area that is about one-tenth that of the diaphragm itself, resulting in a pressure-volume velocity transformation ratio of ten-to-one between the diaphragm and the exit of the phasing plug. It is this mechanical-to-acoustical transformation action that effectively matches the driver's diaphragm impedance to that at the throat of the horn.

### 7.3 Analysis of compression drivers

Figure 7-7A shows a simplified section view of a portion of a WE-type phasing plug with details of diaphragm spacing, slit spacing, and slit width. Using this representation as a starting point, Wentz and Thuras (1934), described the acoustical impedance of the diaphragm as seen at the phasing plug. Using the terminology shown at *A*,  $2W$  is the slit width,  $H$  is the diaphragm-to-phasing plug spacing, and  $L$  is the center-to-center spacing between adjacent annular slits. Figure 7-7B and *C* show the resulting diaphragm acoustical resistive and reactive impedance values corresponding to the  $H/W$  ratios shown at *A*.

The quantity  $2L$  in Figure 7-7A is the spacing between adjacent slits in the phasing plug, and it determines the reference frequency in the graphs. For example, if the spacing between adjacent slits in the phasing is 12 mm (a typical value), the corresponding frequency for the 0.1 marker along the horizontal axis is approximately 700 Hz, and the frequency corresponding to 1.0 is 7 kHz. It is clear from Figure 7-7B and *C* that optimum response is obtained at curve 2, where the  $H/W$  ratio is equal to  $2/3$ . While curve 1 would seem a better choice for extended frequency response, note that it would lead to lower overall driver sensitivity and/or lower diaphragm excursion capability, due to the closer spacing of the diaphragm to the phasing plug.

Virtually all professional compression drivers built from the 1930s to the present time have made use of the basic diaphragm-phasing plug relationships developed by Wentz and Thuras. Variations and improvements have been based largely on diaphragm construction, adhesives and magnet materials.

Working some 45 years later – and an octave higher in frequency response – Locanthi and Kinoshita (1978) essentially validated the earlier analysis. Using the equivalent circuit shown in Figure 7-8A, they produced families of response curves in which the exact roles of several design parameters were

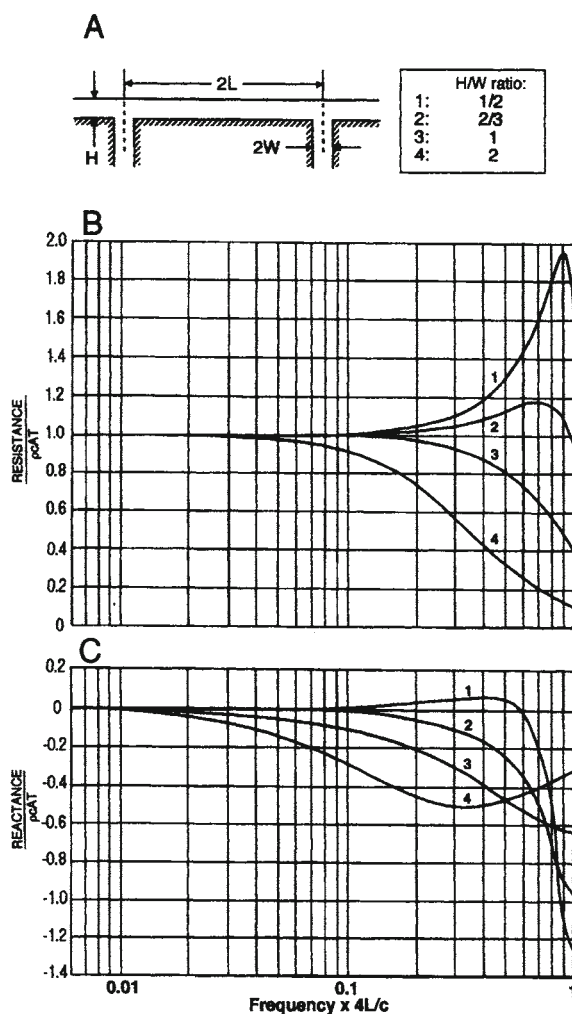


Figure 7-7. Wentz's analysis of compression drivers. Basic model (A); response (B). (Data after Wentz and Thuras, 1934)

individually optimized in producing highest efficiency. Their findings are summarized as follows:

1. The  $Bl$  product should be as large as practicable (see Figure 7-8B).
2. The diaphragm-to-phasing plug spacing should be as small as possible, consistent with excursion demands (see Figure 7-8C).
3. Diaphragm moving mass should be as small as possible (see Figure 7-8D).
4. The spacing between phasing plug slits should be as large as possible, consistent with maintaining the desired HF power response extension.

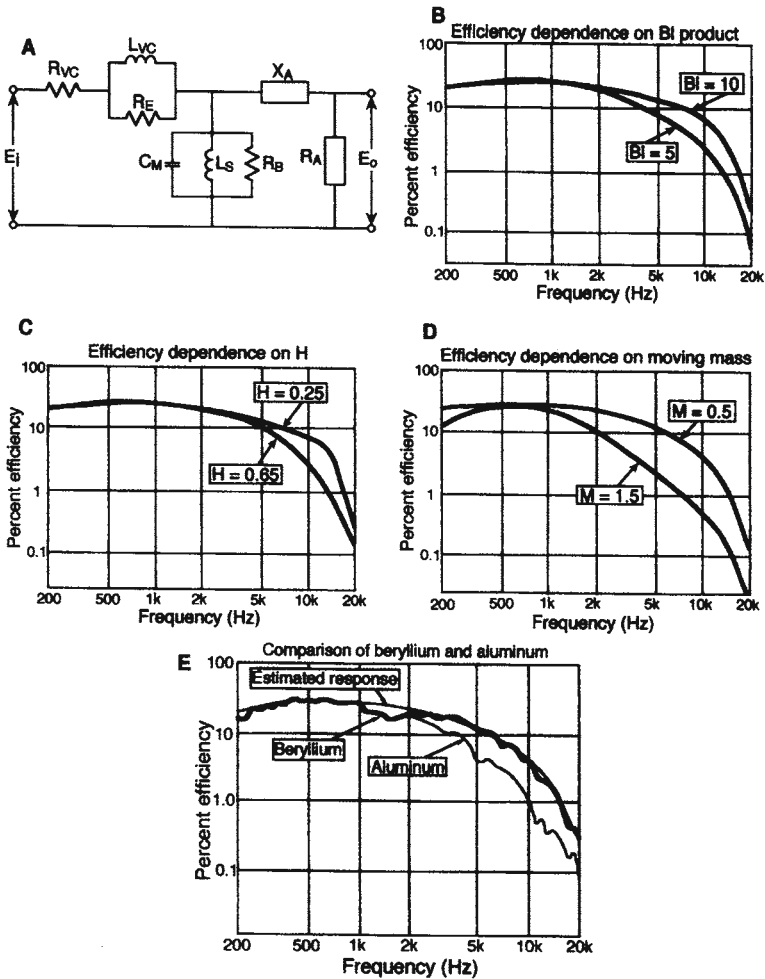


Figure 7-8. Compression driver analysis. Equivalent circuit (A); effects of parameter variations (B through E). (Data after Kinoshita and Locanthi, 1978)

5. The ratio of diaphragm area to slit area has little effect on efficiency, but a high ratio reduces peak excursion requirements for a given output, while increasing second harmonic distortion.

In summary, the authors state that the most important factors in obtaining the flattest and most extended HF response are low diaphragm mass and high  $BI$  product. This quest for ultimate performance leads to beryllium as the material of choice for diaphragms (because of its high stiffness and low mass), and to high saturation alloys in magnet assemblies. Both of these options are expensive, but well worth the investment for ultimate performance. The

measured difference between beryllium and aluminum diaphragms is shown in Figure 7-8E.

During the same period, Murray and Keele at JBL arrived at a set of equations that defined the broad parameters of compression driver mid-band response. An analogous circuit for the driver, loaded by a horn, is shown in Figure 7-9A. On the mechanical and acoustical side, the circuit is of the mobility type, where  $M_{MS}$  is the mass of the moving system (diaphragm and voice coil).  $C_{MS}$  is the mechanical compliance and  $C_{MB}$  is the compliance of the air space behind the diaphragm;  $r_{MS}$  and  $r_{MB}$  are their associated values of mechanical responsiveness.  $C_{M1}$  is the compliance of the small (but by no means insignificant) air space between the diaphragm and the phasing plug.

In the normal passband of the driver we can simplify this equivalent circuit, reflecting it back to the electrical side as shown in Figure 7-9B. Here,  $R_E$  represents the electrical resistance in the amplifier-voice coil circuit and  $R_{ET}$  represents the effective radiation resistance in ohms reflected through the mechanical and acoustical systems:

$$R_{ET} = S_T(B1)^2/\rho_0 c S_D^2 \quad 7.5$$

If a driver has been designed for flattest response, then  $R_E$  and  $R_{ET}$  will both be just about equal, and the efficiency will be:

$$\text{Efficiency (\%)} = [2 R_E R_{ET} / (R_E + R_{ET})^2] \times 100 \quad 7.6$$

This value will be 50% when  $R_E$  and  $R_{ET}$  are equal.

At high frequencies, the equivalent electrical circuit is as shown in Figure 7-9C. The additional reactive elements affect the frequency response by progressively rolling off high frequency response.  $L_E$  represents the inductance of the voice coil, and its effect can always be seen in the impedance curve of the driver as a rise in impedance at higher frequencies. Some driver manufacturers deposit a thin copper or silver ring on the polepiece, which minimizes the rise in impedance due to the coil's inductance by acting as a transformer with a shorted secondary turn.

$C_{MES}$  is a shunt capacitance which causes the so-called *mass breakpoint* in the driver's frequency response. This is a 6 dB/octave roll-off in high frequency response commencing at  $f_{HM}$ :



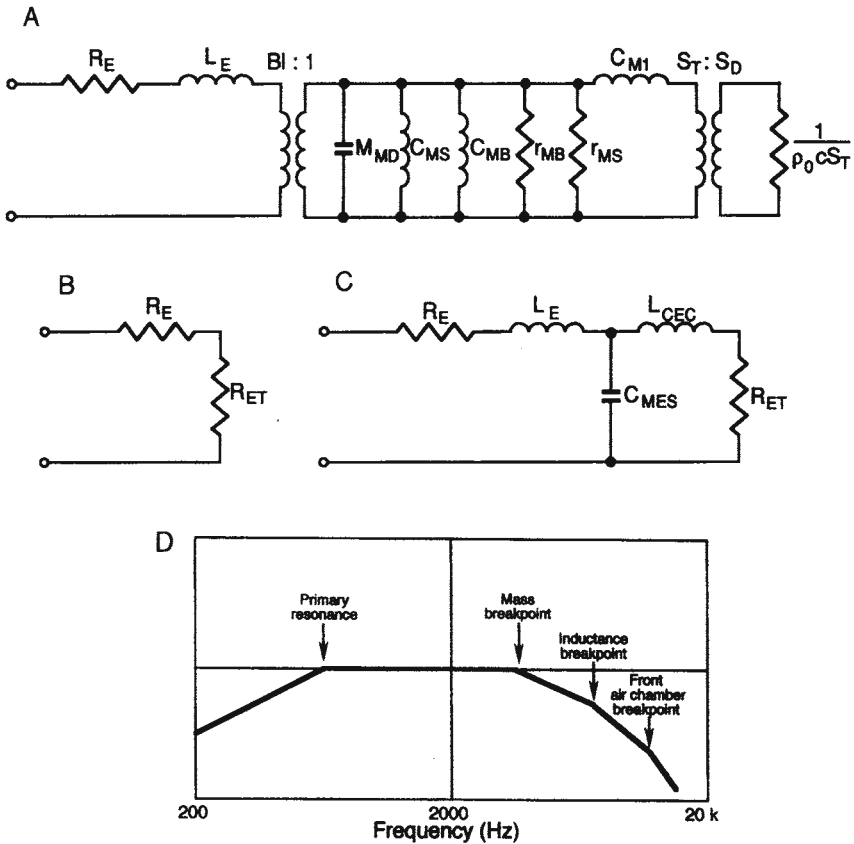


Figure 7-9. Equivalent circuit of a compression driver (A); simplified circuit for MF operation (B); simplified circuit for HF operation (C); response (D).

$$f_{HM} = (BI)^2 / \pi R_E M_{MS} \quad 7.7$$

The mass breakpoint is significant in all traditional high frequency compression driver designs and normally falls in the range between 3 and 4 kHz.

Finally,  $L_{CEC}$  is a series inductance corresponding to the front air chamber between the diaphragm and phasing plug. In some drivers the effect of the front air chamber may be noticed as low as 8 kHz. For drivers optimized for high frequencies its effect may be negligible.

At low frequencies, the driver's response is limited by the primary diaphragm resonance, and in most high frequency drivers this usually takes

place in the range of 500 Hz. Although a given horn may provide extended resistive loading below the driver's resonance, operating the driver below resonance will call for careful monitoring of signal input. Most manufacturers will state a driver power derating value for such operation. The regimes of response of the compression driver are shown in Figure 7-9D.

We should note that the mid-band efficiency of a compression driver, when measured on a typical horn, may be 1 to 1.5 dB lower than that measured on a PWT. The insertion loss is due primarily to slight acoustical impedance differences between the two loading conditions.

### *7.3.1 Calculations of driver performance*

As examples of performance calculations based on driver parameters, we will use the JBL 2441J compression driver:

$Bl = 17 \text{ Tm}$  (gap flux density times coil length)

$M_{MS} = 3.3 \text{ g}$  (mass of moving system)

$f_s = 500 \text{ Hz}$  (resonance frequency of moving system)

$S = 32.5 \times 10^3 \text{ N/m}$  (restoring force of compliance, newtons per meter)

$\omega = (S/M)^{0.5}$  ( $2\pi$  times resonance frequency)

Force ( $f$ ) =  $S \times \text{displacement}$  (force on moving system)

Voice coil diameter = 4 in

Number of turns in voice coil = 30

$B = 2.0 \text{ T}$

$R_{DC} = 7.1 \text{ ohms}$  (dc resistance of voice coil)

#### *Maximum displacement:*

Assume a spacing of 0.55 mm between voice coil and phasing plug. Then, the maximum possible force is:

$$f = (32.5 \times 10^4)(5 \times 10^{-4}) = 16.25 \text{ N}$$

Now, force =  $Bl i$ , so

$i = 16.25/17 = 0.96 \text{ amperes}$ , peak current

$i = (0.96)(0.707) = 0.68 \text{ rms current}$ .

Power =  $i^2 R$ , and if

$R = Z_{min} = 12 \text{ ohms}$

then power = 5.5 watts

Note: This condition exists at very low frequencies and is an indication of how little power is required to reach mechanical limits in a compression driver in that frequency range.

*Maximum diaphragm acceleration:*

power rating of driver = 35 watts, continuous sine wave (with 3-dB crest factor)

therefore: peak power = 70 watts

$Z = 16$  ohms

$W = I^2 R$ , and

$I = (W/Z)^{0.5} = (70/16)^{0.5} = 2.1$  amperes peak current

$Bl = 17$  N/A

peak force =  $17 \times 2.1 = 35.7$  newtons

moving mass of 2441 driver = 0.0033 kg, and  $1 \text{ N} = 1 \text{ kg-m/s}^2$

therefore:  $35.7/0.0033 = 10,818 \text{ m/s}^2$  maximum acceleration

since  $1 \text{ G} = 9.8 \text{ m/s}^2$ ,

maximum acceleration =  $10,818/9.8 = 1103 \text{ G's}$ , or 1103 times the acceleration of gravity.

*Peak acceleration at 2441 driver thermal limit:*

rating of the driver:      75 watts, continuous sine wave  
                                      150 watts, continuous program  
                                      300 watts, program peak

With a pink noise input (6-dB crest factor), the diaphragm undergoes 600 watts of instantaneous power input:

$(600/70)(1103) = 9454 \text{ G}$ , or approximately 10,000 G's peak acceleration.

#### *7.4 The plane wave tube (PWT)*

In carrying out compression driver development, engineers normally measure the driver's response on a plane wave tube (PWT) rather than a horn. Figure 7-10 shows details of the PWT. The tube is normally of the same diameter as the exit of the driver, and a probe microphone is placed fairly close to the mounting flange for the driver. There is a loss of acoustical power as sound progresses down the tube which is caused by a tapered wedge of fiberglass or other suitable damping material. The tube may be 2 or 3 meters in length, and by the time sound has propagated over that distance, it has become attenuated

to such a point that there is little acoustical power to reflect back to the microphone. Acoustically, the tube presents a resistive load to the driver such as would be presented by an infinite horn with a cutoff frequency of zero Hz.

The upper useful frequency of a PWT is given as  $1.22(c/d)$ , where  $c$  is the speed of sound and  $d$  is the diameter of the tube, both given in the same units. Thus, for a PWT with a diameter of 25.4 mm (1 in), the upper frequency limit is 16.5 kHz. The lower frequency limit of a PWT is given as  $c/4l$ , where  $c$  is the speed of sound and  $l$  is the length of the tube, both given in the same units. Thus, a tube 2 meters long would provide reliable data down to about 43 Hz.

It is clear that measuring a 51-mm (2 in) exit driver on a matching PWT would only give reliable HF data up to about 8 kHz. However, many such drivers are routinely capable of response well beyond that frequency, and tapered driver inserts are often used in order to measure the frequency response of larger drivers on smaller tubes.

However, when measuring at absolute midband sensitivity of the driver, a matching diameter PWT should be used. The reason for this is that the acoustical impedance seen by the driver is equal to  $\rho c_0$  times the PWT cross-section area, and the area difference between 25.4 and 51 mm diameter tubes is significant.

The sound pressure level in the PWT is uniform in the portion ahead of the damping material and is equal to:

$$L_p = 94 + 20 \log \sqrt{W_A (\rho_0 c) / S_T} \quad 7.8$$

where  $W_A$  is the acoustical power in watts delivered by the driver and  $S_T$  is the cross-section area of the tube in square meters. Most manufacturers normalize their PWT data to a standard tube with a diameter of 25.4 mm (1 in). Let us now put one watt of acoustical power into such a tube and calculate the value of  $L_p$ :

$$L_p = 94 + 20 \log [(1)406/0.0005]^{0.5}$$

$$L_p = 94 + 20 \log (901) = 94 + 59 = 153 \text{ dB}$$

As a rule, a reference power of 1 milliwatt is used, producing a level of 123 dB in the tube.

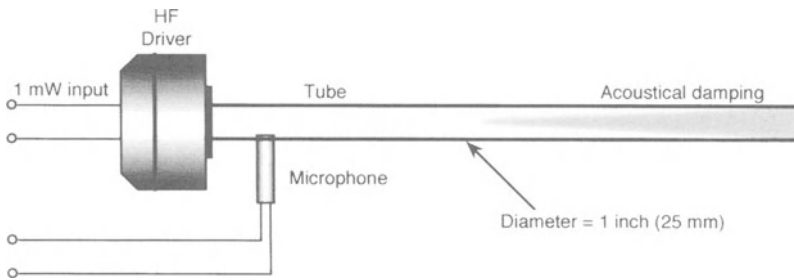


Figure 7-10. Section view of a plane wave tube (PWT).

Figure 7-11 shows typical 1 milliwatt PWT response of a JBL 2446 compression driver. Note that the maximum level in the pass-band of the driver is 119 dB  $L_p$ . This value is 4 dB lower than the 1 mW reference level of 123 dB  $L_p$ , indicating that the driver's efficiency is  $100 \times 10^{-4/10}$ , or 40%.

We can also see the effect of the mass breakpoint in the driver's response in the 3.5 kHz range. We can compare this with the value given by equation 7.7:

$$Bl = 18 \text{ Tm}$$

$$R_E = 8.5 \text{ ohms}$$

$$M = 0.00346 \text{ kg}$$

$$f_{HM} = (18)^2 / \pi (8.5) (0.00346) = 3507 \text{ Hz}$$

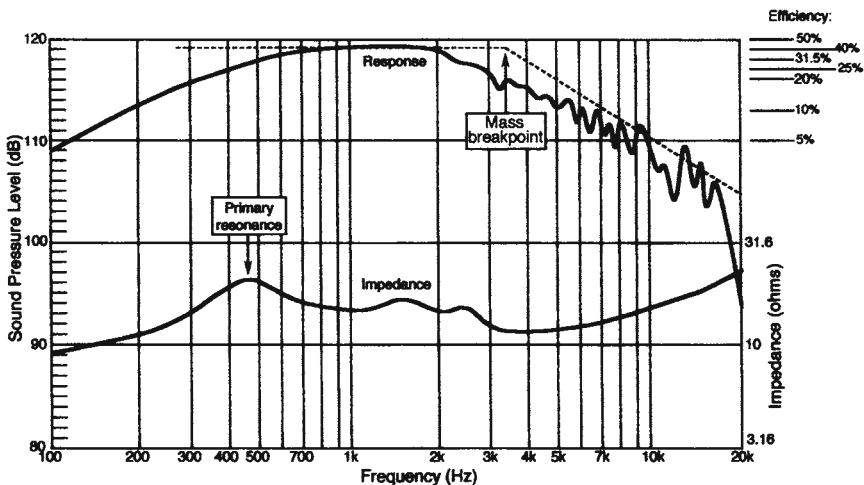


Figure 7-11. Plots of amplitude response and impedance for JBL 2445J driver on PWT. (Data courtesy JBL)

On the graph, a breakpoint at 3500 Hz has been superimposed by dotted lines over the response curve. Note that it effectively matches the transition point in the curve.

The modulus of impedance of the driver has been plotted below the response curve, and the driver's primary resonance at about 500 Hz is obvious.

### 7.5 Secondary resonances in the compression driver

Our analysis thus far has assumed that the driver's diaphragm moves as a unit. At high frequencies, more complex motion occurs and may have a profound effect on response. There is, in most drivers, a secondary resonance that occurs in the surround, or suspension, of the driver. When this resonance takes place, motion from the voice coil causes considerable motion in the surround itself and relatively little in the diaphragm.

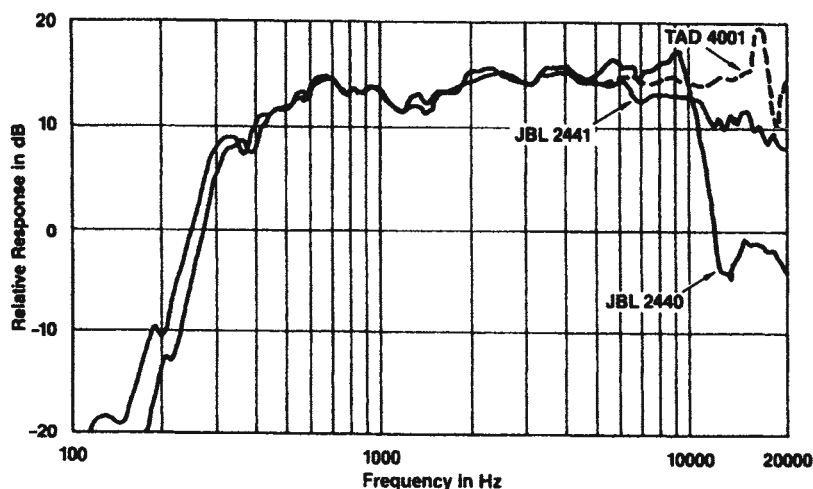


Figure 7-12. Response of three drivers mounted on JBL 2350 radial horn. (Data courtesy JBL)

Figure 7-12 shows superimposed response curves of three drivers mounted on a JBL 2350 radial horn. The curves are unequalized, and two of them (JBL 2440 and TAD 4001) show the effect of secondary resonances in their half-roll surrounds. The elevated response of the 2440 driver at 9 kHz and at 17 kHz in the 4001 driver are due to secondary resonances at those frequencies. The beryllium diaphragm in the 4001 driver is considerably stiffer than the aluminum diaphragm in the 2440, and this accounts for the shift of nearly an octave in its secondary resonance. By comparison, the 2441 diaphragm design has a *diamond* surround treatment (see Figure 7-6C) that distributes secondary

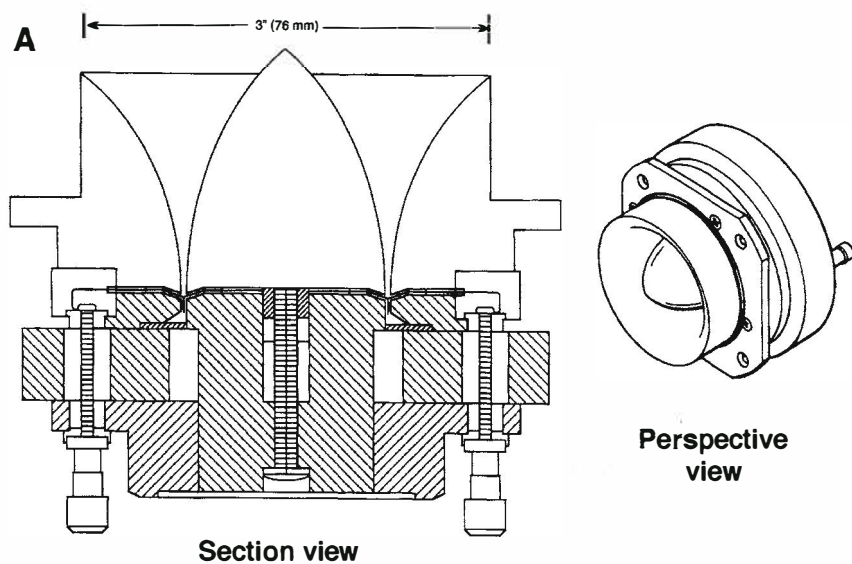
resonances, providing a smoother overall curve, but one that has more apparent roll-off than the other two in the range between 5 and 10 kHz. These response curves are typical of the many design factors and trade-offs that the transducer engineer must deal with.

### *7.6 Ring radiators and UHF drivers*

Ring radiators are very high frequency devices operating normally in the range from about 4 kHz to 20 kHz. They embody the elements of a compression driver and horn in a single unit. Section and perspective views of the JBL 2402 ring radiator, often called the “bullet,” are shown in Figure 7-13. The diaphragm is clamped at the outer edge as well as in the middle, effectively forming an annular, or ring shaped, radiating surface. The initial horn flare is annular in shape, eventually making a transition to a horn with a circular cross-section. Other models of the ring radiator have the same basic driving mechanism but with different horn configurations.

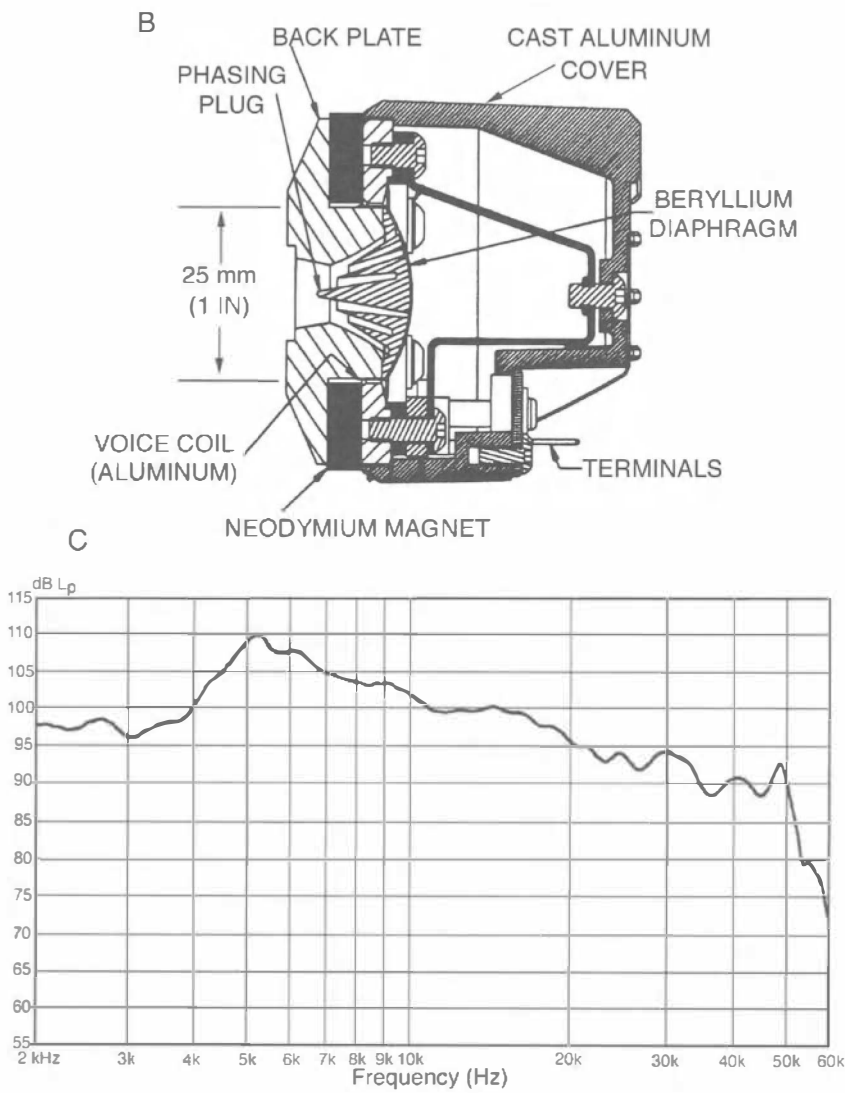
Over their operating range, ring radiators can exhibit efficiencies on the order of 6.3% and handle peak power inputs of up to 40 watts, yielding a power output, per device, of about 2.5 acoustic watts. They are often used in multiple arrays for greater output capability.

Figure 7-13B shows a section view of the JBL Be045 compression driver, which is designed to cover the frequency range from 10 kHz to 50 kHz. The driver has a 25-mm (1 in) diameter phasing plug and is used in monitoring high-resolution digital recordings. The driver is normally used above 10 kHz, and typical frequency response is shown at C.



**Figure 7-13.** Section and perspective views of JBL 2402 ring radiator (A); section view (B) and 1-meter on-axis response (C) of JBL 045Be UHF driver. (Data courtesy JBL)





**Figure 7-13. Continued.**